Photocatalysis oxidative desulfurization of dibenzothiophene in extremely deep liquid fuels on the Z-scheme catalyst of ZnO-CuInS_2-ZnS intelligently integrated with carbon quantum dots: Performance, mechanism, and stability†

Manh B. Nguyen

Institute of Chemistry, Vietnam Academy of Science and Technology, 18 Hoang Quoc Viet, Cau Giay, Hanoi, Viet Nam. Email: nguyenbamanh@ich.vast.vn

Table S1. Characterization

The morphology of both ZnO, CuInS_2, ZnS, ZCZ and ZCZ-CQD materials was examined by transmission electron microscopy (TEM) with an acceleration voltage of 200 kV (Leica IEO 906E). X-ray diffraction (XRD) analysis was conducted using a D8 Advance X-ray diffractometer (Bruker, Germany) equipped with a CuKα radiation source (2θ range ~ 5–50° and λ = 0.154 06 nm). Elemental composition was determined by energy-dispersive X-ray spectroscopy (EDS) using a JEOL JED-2300 energy-dispersive spectrometer. The specific surface area was measured using a Tristar-3030 system (Micromeretics-USA) with N_2 adsorption at 77 K employing the Brunauer-Emmett-Teller (BET) method. X-ray photoelectron spectroscopy (XPS) was performed using a Thermo VG Multilab 2000 instrument. Photoluminescence (PL) and UV-vis diffuse reflectance spectroscopy (DRS) were recorded on a Cary Eclipse fluorescence spectrophotometer (Varian) and a UV-2600 spectrophotometer (Shimadzu), respectively.

Scavenging experiments of reaction radicals involve adding 2 mM of hydroxyl radical scavengers, p-benzoquinone (p-BQ), superoxide radical scavengers, ammonium oxalate monohydrate (AO) into the reaction system before light irradiation.

Table S1. Elemental composition (wt%) of ZnO, CuInS2, ZnS and ZCZ-CQD samples

Materials	Zn	O	Cu	In	S	C	N	Total
ZnO	76.52	23.48	-	-	-	-	-	100
CuInS_2	-	-	25.8	48.69	25.51	-	-	100
ZnS	65.97	-		-	34.03	-	-	100
ZCZ-CQD	47.28	6.38	6.29	14.24	22.16	2.7	0.95	100

Table S2. Binding energies of the bonds in the ZnO, $CuInS_2$, ZnS and ZCZ-CQD samples

	Materials	**ZnO**	**$CuInS_2$**	**ZnS**	**ZCZ-CQD**	**ZCZ-CQD after reaction**
Zn2p	Zn $2p_{3/2}$	1021.57	-	1021.64	1021.86	1021.99
	Zn $2p_{1/2}$	1044.66	-	1044.77	1044.94	1045.07
O1s	C=C/C–O	-	-	-	530.22	530.77
	Zn–O	531.22	-	-	531.57	531.96
	–OH	532.77	-	-	532.36	533.00
S2p	$S2p_{3/2}$	-	161.59	161.50	161.54	161.83
	$S2p_{1/2}$	-	163.26	163.08	163.16	163.40
Cu2p	Cu^{+}	-	932.04	-	931.56	931.75
		-	951.81	-	951.50	951.57
	Cu^{2+}	-	933.17	-	932.85	933.19
		-	953.19	-	952.93	953.26
In3d	In^{2+}	-	444.95	-	444.63	445.44
		-	452.58	-	452.22	453.01
	In^{3+}	-	445.74	-	445.37	445.90
		-	453.12	-	452.86	453.47
C1s	C–C/C=C	-	-	-	284.77	284.92
	C–O	-	-	-	286.31	286.44
	C=O	-	-	-	288.40	288.92

Table 3. Comparison of different photocatalysts in the DBT degradation process

Materials	Reaction conditions	Light source	Photocatalytic performance (%)	Time (min)	Ref.
ZCZ-CQD	$m_{catalyst}$ = 1.5 g/L [DBT] = 300 mg/L,	300 W Xe lamp	98.32	120	This work
α-Fe_2O_3/g-C_3N_4/HNTs	$m_{catalyst}$ = 2.5 g/L [DBT] = 200 mg/L	300 W Xe lamp	96.01	180	[1]
AgCl/$PbMoO_4$	$m_{catalyst}$ = 1.5 g/L [DBT] = 200 mg/L	-	97.0	120	[2]
Ag-AgBr/Al-MCM-41	$m_{catalyst}$ = 2.0 g/L [DBT] = 500 mg/L,	125 W high-pressure Hg	98	360	[3]
Ni-WO_3@g-C_3N_4	$m_{catalyst}$ = 2.0 g/L [DBT] = 100 mg/L	-	97.0	180	[4]
CeO_2/ATP/g-C_3N_4	[DBT] = 200 mg/L	300 W Xe lamp	98	180	[5]

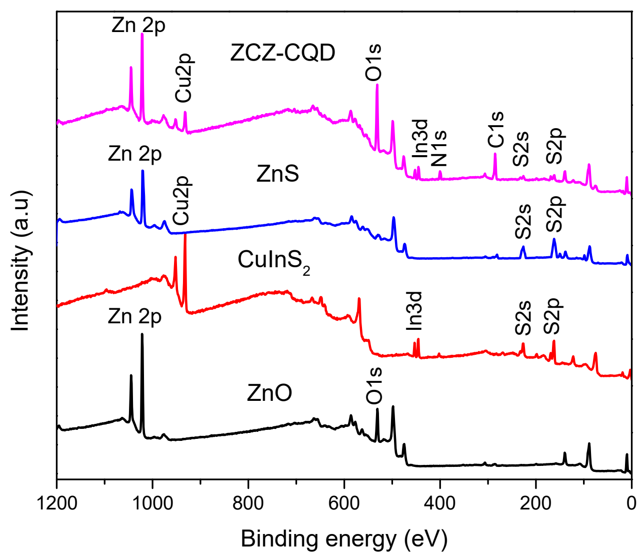

Figure S1. Full scan XPS spectra of ZnO, $CuInS_2$, ZnS and ZCZ-CQD samples

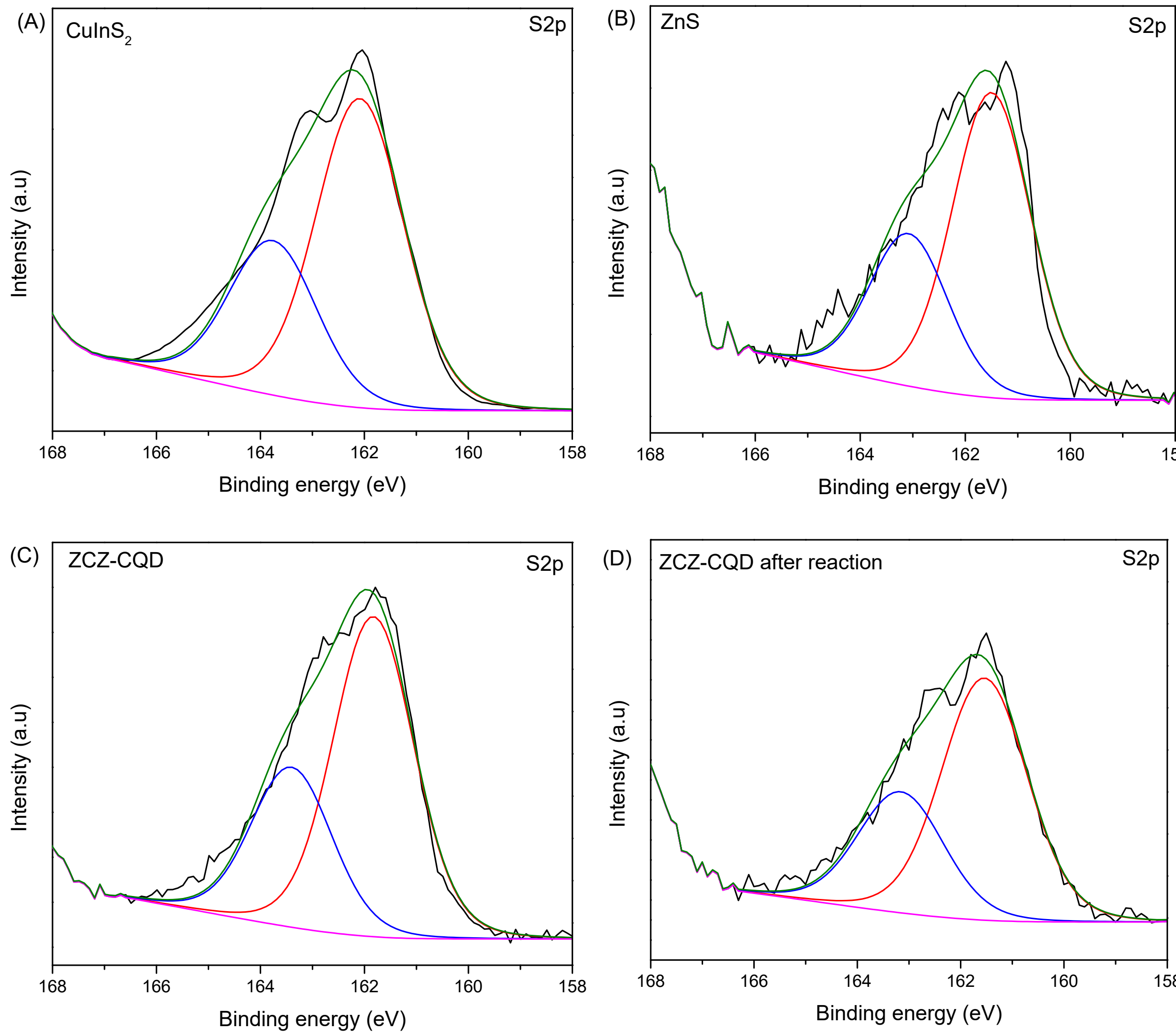

Figure S2. High-resolution S 2p XPS spectra of $CuInS_2$ (A) ZnS (B) and ZCZ-CQD (C) and CZC-CQD after 10 cycles (D)

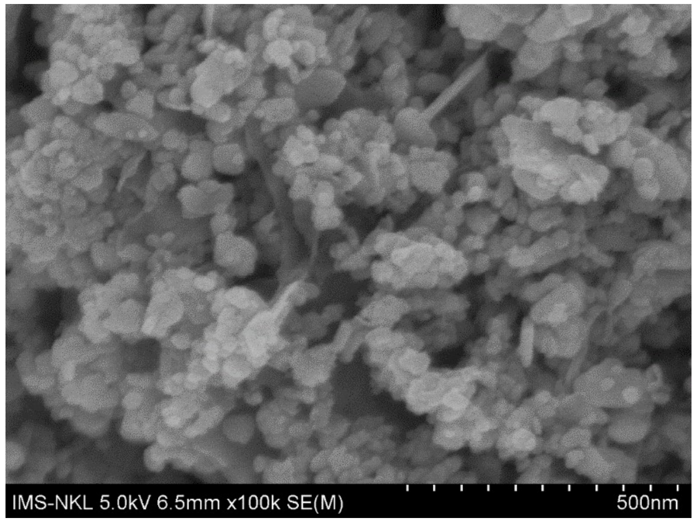

Figure S3. SEM image of ZCZ-CQD sample

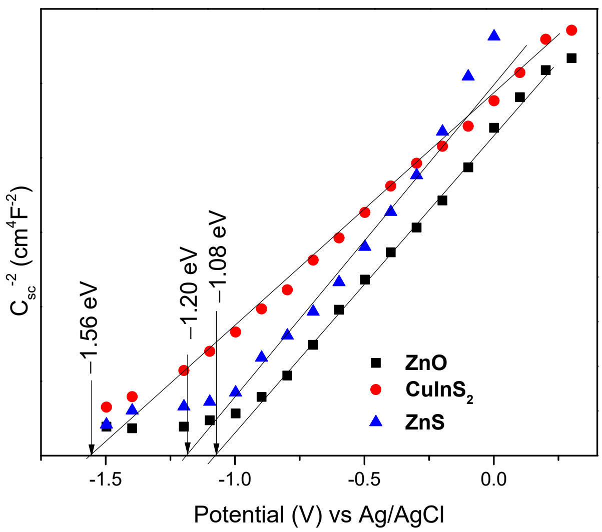

Figure S4. Mott-schotky plot of ZnO, $CuInS_2$ and ZnS samples

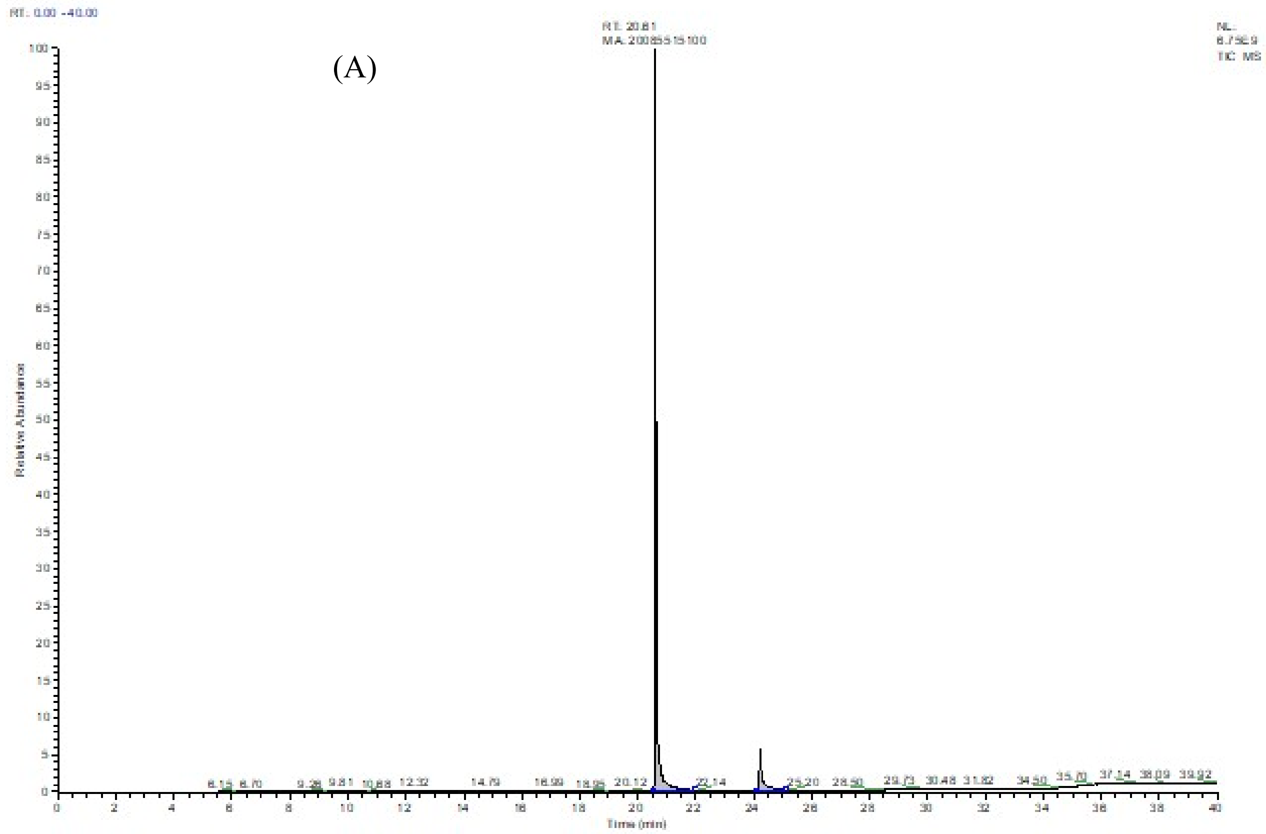
(A)
RT: 0.00 - 40.00
RT: 20.81
MA: 20085515100
TIC MS 1
Relative Abundance
Time (min)

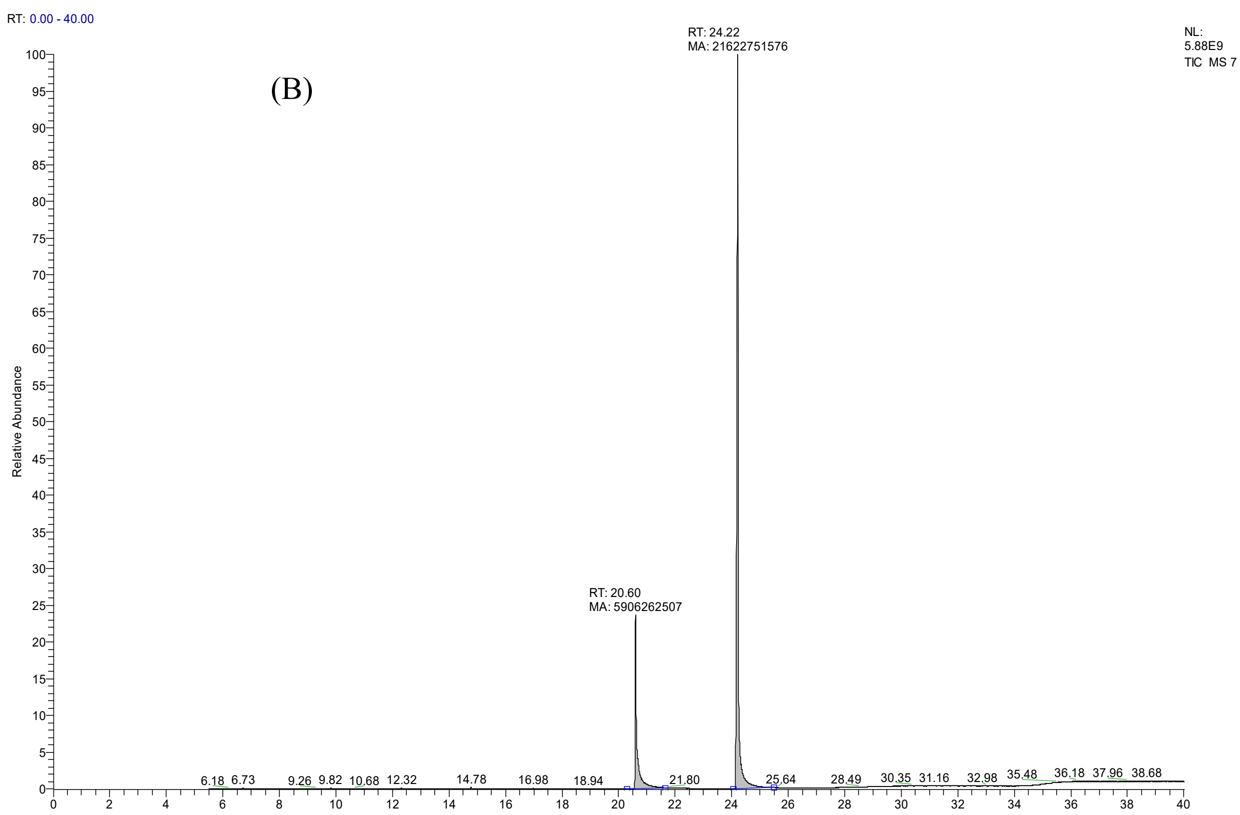
(B)
RT: 0.00 - 40.00
RT: 24.22
MA: 21622751576
NL:
5.88E9
TIC MS 7
RT: 20.60
MA: 5906262507
6.18
6.73
9.26
9.82
10.68
12.32
14.78
16.98
18.94
21.80
25.64
28.49
30.35
31.16
32.98
35.48
36.18
37.96
38.68
Relative Abundance
Time (min)

Figure S5. GC-MS of DBT (A) GC-MS spectra of the products in the desulfurization of DBT over ZCZ-CQD photocatalyst after 10 min

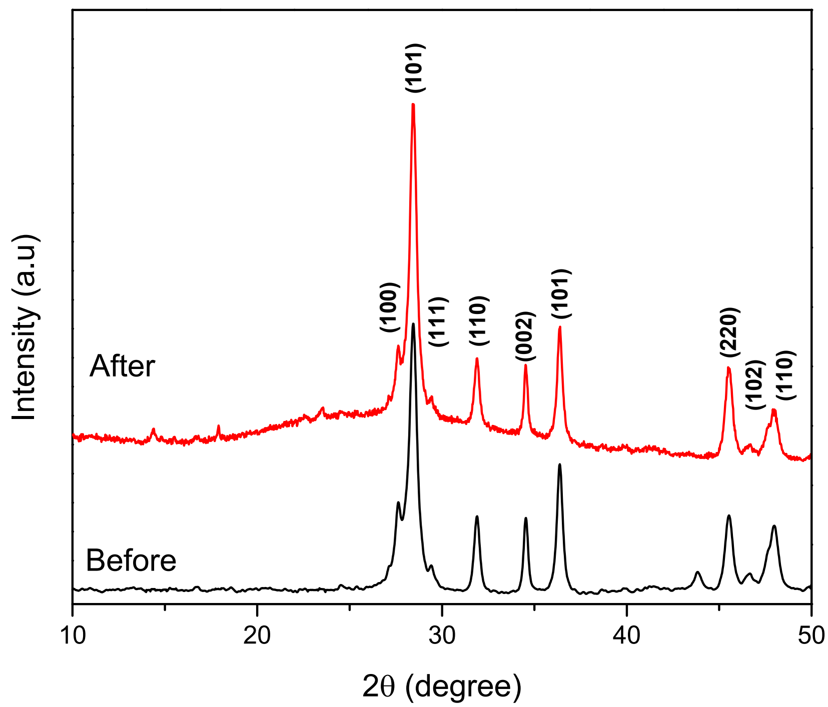

Figure S6. XRD patterns of ZCZ-CQD before and after 10 cycles reaction

References

(1) Zhou, X.; Liu, H.; Liu, S.; zhang, L.; Wang, T.; Wang, C.; Su, D. Constructing Efficient α-Fe2O3/g-C3N4/HNTs-Loaded Heterojunction Photocatalysts for Photocatalytic Oxidative Desulfurization: Influencing Factors, Kinetics, and Mechanism. *Fuel* **2023**, *332* (P1), 126147. https://doi.org/10.1016/j.fuel.2022.126147.

(2) Chang, H.; Yi, H.; Ke, Q.; Zhang, J. Preparation of a AgCl/PbMoO4 Composite and Investigation of Its Photocatalytic Oxidative Desulfurization Performance. *ACS Omega* **2020**, *5* (19), 10927–10938. https://doi.org/10.1021/acsomega.0c00695.

(3) Pham, X. N.; Nguyen, B. M.; Thi, H. T.; Van Doan, H. Synthesis of Ag-AgBr/Al-MCM-41 Nanocomposite and Its Application in Photocatalytic Oxidative Desulfurization of Dibenzothiophene. *Advanced Powder Technology* **2018**. https://doi.org/10.1016/j.apt.2018.04.019.

(4) Saeed, M.; Munir, M.; Intisar, A.; Waseem, A. Facile Synthesis of a Novel Ni-WO3@g-C3N4Nanocomposite for Efficient Oxidative Desulfurization of Both Model and Real Fuel. *ACS Omega* **2022**, *2*. https://doi.org/10.1021/acsomega.2c00886.

(5) Li, X.; Zhu, W.; Lu, X.; Zuo, S.; Yao, C.; Ni, C. Integrated Nanostructures of

CeO2/Attapulgite/g-C3N4 as Efficient Catalyst for Photocatalytic Desulfurization: Mechanism, Kinetics and Influencing Factors. *Chemical Engineering Journal* **2017**, *326*, 87–98. https://doi.org/10.1016/j.cej.2017.05.131.